

HarDNet-MSEG: A Simple Encoder-Decoder Polyp Segmentation Neural Network that Achieves over 0.9 Mean Dice and 86 FPS

Chien-Hsiang Huang , Hung-Yu Wu , and Youn-Long Lin

Department of Computer Science, National Tsing Hua University
 {james128333, a9778875}@gmail.com, ylin@cs.nthu.edu.tw

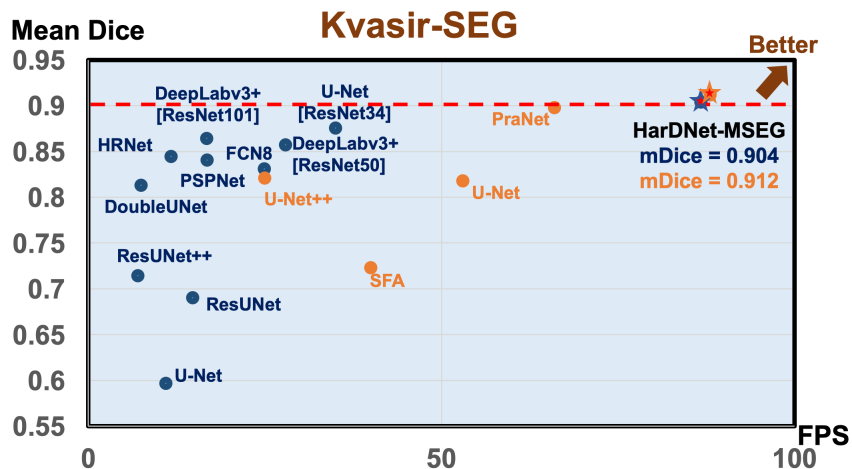


Figure 1: Mean Dice accuracy vs frame rate running on a GeForce RTX 2080 Ti GPU as reported in [20](blue) and [13](orange). HarDNet-MSEG is faster and more accurate than the SOTA (U-Net[ResNet34] and PraNet).

Abstract

We propose a new convolution neural network called HarDNet-MSEG for polyp segmentation. It achieves the SOTA in both accuracy and inference speed on five popular datasets (Kvasir-SEG[22], CVC-ColonDB[19], EndoScene[31], ETIS-Larib Polyp DB[30] and CVC-Clinic DB[5]). For Kvasir-SEG, HarDNet-MSEG delivers **0.904 mean Dice** running at **86.7**

FPS on a GeForce RTX 2080 Ti GPU (showing in Figure 1). It consists of a backbone and a decoder. The backbone is a low memory traffic CNN called HarDNet68[7], which has been successfully applied to various CV tasks including image classification, object detection, multi-object tracking ,and semantic segmentation, etc. The decoder part is inspired by the Cascaded Partial Decoder[32], known for fast and accurate salient object detection. We have evaluated HarDNet-MSEG using those five popular datasets. The code and all experiment details are available at Github. <https://github.com/james128333/HarDNet-MSEG>

1 Introduction

The incidence of colorectal cancer (CRC) has been ranked third in the world for many years. Therefore, how to prevent CRC is an important global issue. Studies have pointed out that 95% of CRC is due to a colorectal adenomatous polyp. The resection of colorectal adenomatous polyps can greatly reduce the incidence of CRC. Therefore, it is very important to have a colonoscopy on a regular basis as well as early invention and treatment.

At present, the best way to prevent CRC is by taking regular colonoscopy and undergo a polyp removal resection. With the emergence and popularization of painless colonoscopy, people’s acceptance of the examination is getting higher. However, the detection of polyps was performed manually by endoscopists in the past, which is a consuming task for human beings and greatly depends on the doctor’s experience and ability. Early segmentation methods[2, 19, 4] are based on extracting features such as color, patterns, etc., and then using a classifier to distinguish polyps from their surroundings. However, this method still has a high rate of missed detection. The position, size, color, etc. of each polyp are different, so it is very difficult to segment them automatically and accurately.

In recent years, CNN has grown rapidly with breakthrough growth in the application of various imaging tasks. The segmentation of polyp have also benefited[6, 1]. For this task, FCN[27, 6, 1], U-Net[28, 29], U-Net++[24, 36], DoubleU-Net[21] and ResUNet[23, 33, 20] series, etc., have good results compared to the early methods. Most polyp blocks can be segmented out well, but there are still many problems, such as the cutting of boundary areas and the lack of smaller blocks, as well as broken images in large areas. Moreover, the inference time of these networks is usually long, and the training time is relatively time-consuming.

We propose HarDNet-MSEG based on the backbone of HarDNet68[7]. With a simple encoder-decoder[3] architecture, it achieves excellent accuracy and efficient inference time for related benchmarks such as Kvasir-SEG, CVC-ColonDB, etc.

2 Related work

Since the emergence of LeNet[25] in 1998, CNN has grown rapidly and has been used in different computer vision fields. Among them, the task of image segmentation is widely used in medical imaging.

In 2015, Long et al. first introduced fully convolutional networks (FCN)[27] for the task of image segmentation. An end-to-end trained convolutional neural network is used to classify each pixel in an image. Since then, the convolutional neural network has flourished in the field of image segmentation. In the same year, U-Net[29] introduced at MICCAI has been widely used in the field of medical imaging. Through a fairly symmetrical U-shaped encoder-decoder architecture, combined with skip connections at different scales to integrate deep and shallow features, it has now become a baseline network architecture for most medical imaging semantic segmentation. Then, the emergence of U-Net++[24, 36] expands the original U-shaped architecture. With more skip connections and convolutions to achieve the effect of deep layer aggregation[34]. It solves the problem that edge information and small objects are easily lost due to deep network down-sampling and up-sampling.

In recent years, the use of a better CNN backbone, or the introduction of additional modules like spatial pyramid pooling[16], attention modules[8, 15], etc., have achieved very good results in medical imaging semantic segmentation. Examples of the former include ResUNet[33, 20], ResUNet++[23], and DoubleU-Net[21]. By integrating a better CNN backbone with a U-shaped structure, the entire network has a stronger recognition capability, a larger receiving domain, and multi-scale information integration. The second is to insert additional modules, such as DoubleU-Net[21] uses ASPP[9] between the encoder and the decoder, which helps to deal with different object scales and improve accuracy; PraNet[13] adds an RFB[26] module to skip connection to capture more visual information for features of different scales. In recent years, attention has also been widely used in the field of computer vision, especially for semantic segmentation which requires detailed edge information at the pixel level. Examples include PraNet[13], PolypSeg[35] and ABC-Net[14]. After adding different context modules, they all get good results in medical imaging segmentation. Context modules such as Spatial Attention Module[10] and Channel Attention Module[10] will reduce the inference speed, but on the other hand, they are very efficient in improving accuracy and making edge cutting more precise.

The HarDNet-MSEG we proposed uses HarDNet[7] as the backbone and is designed with an encoder-decoder architecture. It has achieved the high accuracy of the current state of the art in CVC-ColonDB, EndoScene, ETIS-Larib Polyp DB, CVCclinic DB, and Kvasir-SEG, and at the same time has an efficient inference speed. In addition, we have also tried to add additional modules such as RFB, ASPP, Attention, etc. to our network architecture to further improve the accuracy.

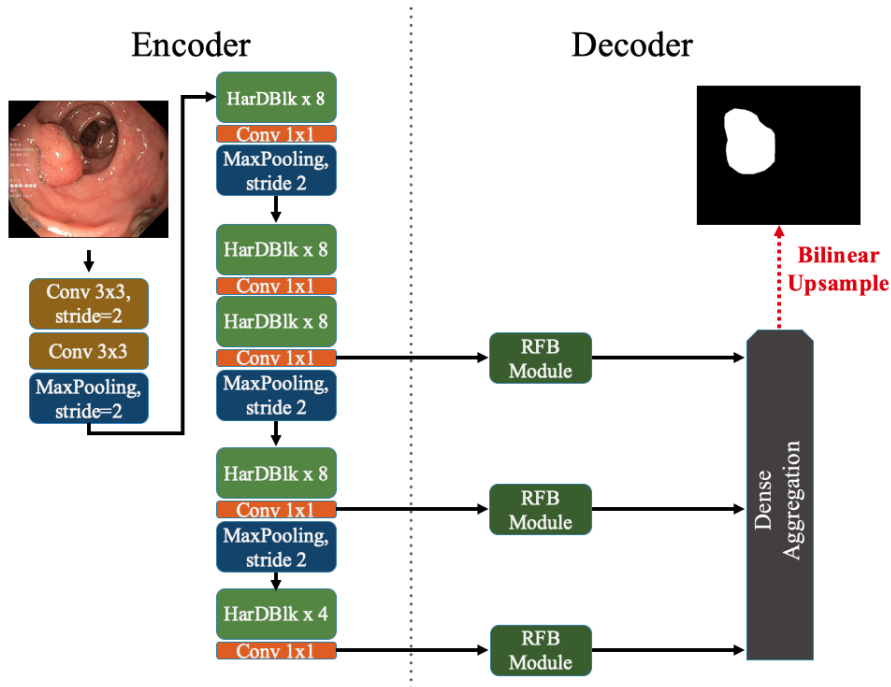


Figure 2: HarDNet-MSEG overview. The encoder part consists of HarDNet68, and the decoder part is using partial decoder.

3 HarDNet-MSEG

Figure 2 depicts the architecture of our proposed HarDNet-MSEG. It consists of an encoder backbone and a decoder.

3.1 Backbone : HarDNet

HarDNet[7], improved the original dense block of Densenet[18] are illustrated in Figure 3. Considering the impact of memory traffic on model design, it reduces shortcuts to increase the inference speed, and at the same time increases its channels' width for the key layer to make up for the loss of accuracy. It also uses a small amount of Conv1x1 to increase computational density.

Through this design, it not only achieves 30% inference time reduction compared with DenseNet[18] and ResNet[17], also having higher accuracy on ImageNet[12]. On the other hand, FC-HarDNet70[18] also reaches the state of the art in image segmentation on Cityscapes Dataset[11]. Therefore, we use

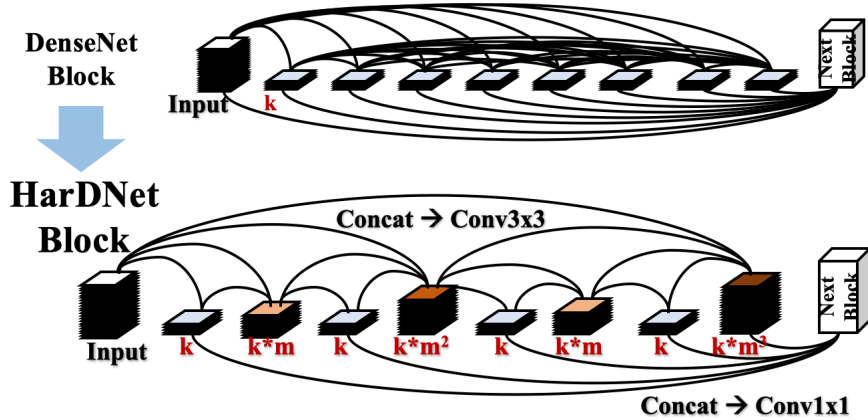


Figure 3: HarDNet Block overview.

HarDNet68 as the model backbone for Colorectal Polyps image semantic segmentation.

3.2 Cascaded Partial Decoder

Many well-known medical image segmentation networks are often modified based on the U-Net. Our design also went in this direction at the beginning. But based on the balance of the inference time and performance, we did not use HarDBlock (HarDBlk) in the Decoder part, which is different from FC-HarDNet.

We reference the Cascaded partial decoder [32]. It found out that the shallow features have high resolution and occupy computing resources, and the deep information can also represent the spatial details of the shallow information relatively well. So we decide to discard the shallow features and do more computing on the deeper layers' features. At the same time, the aggregation of feature maps at different scales can be achieved by adding appropriate convolution and skip connections.

3.2.1 RFB Module

Figure 4 shows a Receptive Field Block[26]. It can strengthen the deep features learned from a lightweight CNN backbone. By using multi-branch with different kernel size convolution and dilated convolution layers, it generates features with the different receptive fields. Afterwards, it applies a 1x1 convolution to merge these features and generate the final representation.

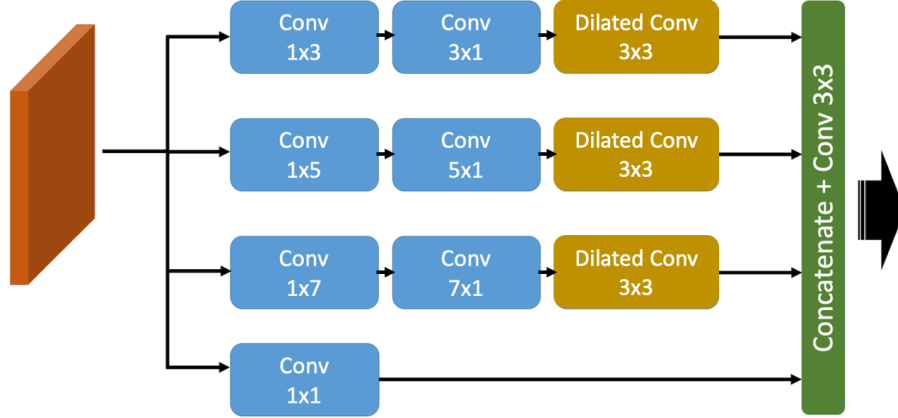


Figure 4: RFB Module overview.

We add this module to the skip connection according to [32], so that we could enlarge our receptive fields from each different resolutions' feature maps.

3.2.2 Dense Aggregation

We perform aggregation by element-wise multiplication shown in Figure 5. After up-sampling to the same scale, the feature is multiplied with another input feature of the corresponding scale.

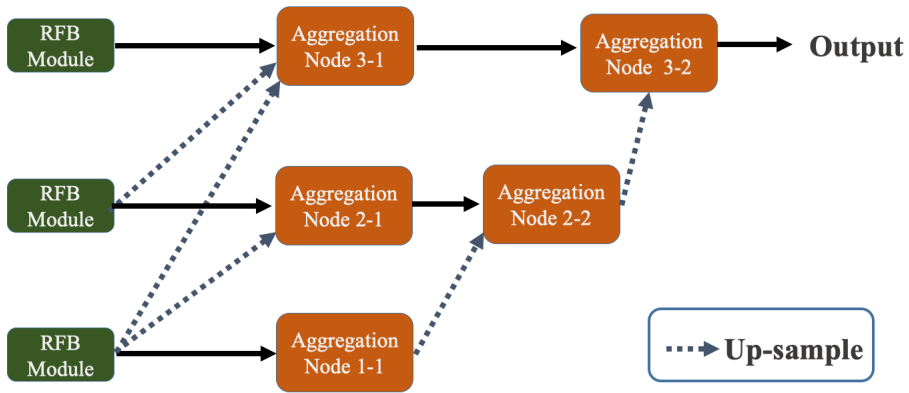


Figure 5: Aggregation Module overview.

4 Experiments

We used the training data from [13] and [20] for training because they have excellent performance in polyp segmentation. The training data and training methods used in the two articles are different. In order to reduce the variable factors, the training methods we use will refer to the methods proposed in the two articles respectively, and then compare the accuracy and inference speed with other models.

	mIoU	mDice	F2-score	Precision	Recall	Overall Acc.	FPS
U-Net	0.471	0.597	0.598	0.672	0.617	0.894	11
ResUNet	0.572	0.690	0.699	0.745	0.725	0.917	15
ResUNet++	0.613	0.714	0.720	0.784	0.742	0.917	7
FCN8	0.737	0.831	0.825	0.882	0.835	0.952	25
HRNet	0.759	0.845	0.847	0.878	0.859	0.952	12
DoubleUNet	0.733	0.813	0.820	0.861	0.840	0.949	7.5
PSPNet	0.744	0.841	0.831	0.890	0.836	0.953	17
DeepLabv3+[ResNet50]	0.776	0.857	0.855	0.891	0.8616	0.961	28
DeepLabv3+[ResNet101]	0.786	0.864	0.857	0.906	0.859	0.961	17
U-Net[ResNet34]	0.810	0.876	0.862	0.944	0.860	0.968	35
HarDNet-MSED	0.848	0.904	0.915	0.907	0.923	0.969	86.7

Table 1: Quantitative results on Kvasir dataset (training/testing split:880/120). Showing the performance of different metrics and inference speed evaluating on GeForce RTX 2080 Ti GPU. Others evaluation scores are refer from [20].

4.1 Dataset

We used the datasets proposed in the two papers mentioned earlier, namely Kvasir-SEG, CVC-ColonDB, EndoScene, ETIS-Larib Polyp DB, and CVC-Clinic DB. And we will make a detailed comparison with other SOTA models on these datasets.

4.2 Training setting and policy

The two articles are based on different splitting method of training data, so we made two different experiments on each training setting to compare, and the details of the experiments will be explained below.

For [20], 880 images of Kvasir-SEG is used for training, and the other 120 images are used for testing. It does use augmentations like random rotation, horizontal flip, vertical flip. Our training input size is 512x512. We train our model with SGD optimizer for 100 epochs and the learning rate is set to 1e-2.

The results comparing to [20] is in Table 1. HarDNet-MSEG shows the greatest accuracy on most metrics, and the inference speed is much faster than others.

In [13], 1450 training images without any augmentation is used, including 900 images in Kvasir-SEG and 550 images in CVC-ClinicDB. And the testing set has 5 datasets mentioned above. Our training input size is 312x312, We train our model with Adam optimizer for 100 epochs and the learning rate is set to 1e-4. The quantitative results of each 5 datasets are shown in Table 2 (Kvasir-SEG) and Table 3 (ETIS, CVC-ClinicDB, CVC-ColonDB and EndoScene). We achieve the best performance in mean Dice and mIoU on each dataset, with the fastest inference speed (88 FPS).

	mDice	mIoU	wfm	Sm	MAE	maxEm	FPS
U-Net	0.818	0.746	0.794	0.858	0.055	0.893	53
U-Net++	0.821	0.743	0.808	0.862	0.048	0.910	25
ResUNet-mod	0.791	n/a	n/a	n/a	n/a	n/a	n/a
ResUNet++	0.813	0.793	n/a	n/a	n/a	n/a	n/a
SFA	0.723	0.611	0.67	0.782	0.075	0.849	40
PraNet	0.898	0.840	0.885	0.915	0.030	0.948	66
HarDNet-MSED	0.912	0.857	0.903	0.923	0.025	0.958	88

Table 2: Quantitative results on Kvasir, comparing with the SOTA. Using the same training script with the release code of PraNet. The inference speed is testing under 312x312 resolution on GeForce RTX 2080 Ti GPU.

	ClinicDB		ColonDB		ETIS		CVC-T	
	mDice	mIoU	mDice	mIoU	mDice	mIoU	mDice	mIoU
U-Net	0.823	0.755	0.512	0.444	0.398	0.335	0.71	0.627
U-Net++	0.794	0.729	0.483	0.410	0.401	0.344	0.707	0.624
ResUNet-mod	0.779	n/a	n/a	n/a	n/a	n/a	n/a	n/a
ResUNet++	0.796	0.796	n/a	n/a	n/a	n/a	n/a	n/a
SFA	0.700	0.607	0.469	0.347	0.297	0.217	0.467	0.329
PraNet	0.899	0.849	0.709	0.640	0.628	0.567	0.871	0.797
HarDNet-MSED	0.932	0.882	0.731	0.660	0.677	0.613	0.887	0.821

Table 3: More results on CVC-ClinicDB, CVC-ColonDB, ETIS, and CVC-T, comparing with the SOTA. Among them, CVC-T is the testing data for EndoScene.

4.3 Metrics

$$\text{Mean Dice} = \frac{2*tp}{2*tp+fp+fn} \quad \text{mIoU} = \frac{tp}{tp+fp+fn}$$

$$\text{Recall} = \frac{tp}{tp+fn} \quad \text{Precision} = \frac{tp}{tp+fp}$$

$$\text{F2} = \frac{5p*r}{4p+r} \quad \text{Acc.} = \frac{tp+tn}{tp+tn+fp+fn}$$

We will mainly use Kvasir’s official website as the basis for comparison, namely mean Dice and Mean IoU, but we will still use other metrics mentioned in these two articles for comparison so that we can show our advantages more clearly.

4.4 Training and Inference Environment setting:

In order to show our advantage in speed, we respectively compare with other famous models. The platforms we use for evaluation is written below.

Intel i9-9900k CPU, GeForce RTX 2080 Ti, Pytorch: 1.6 and CUDA: 10.2

5 Conclusion

HarDNet-MSEG achieved the SOTA in all five challenging datasets. It is the only network that has achieved over 0.90 mean Dice (0.912 comparing with [13] and 0.904 comparing with [20]) on Kvasir-SEG. And it is 1.3 times faster than PraNet and more than 2 times faster than other models. We achieve this with a simple encoder-decoder architecture without any attention module used in [13] and [14]. See Figure 6 for some inference results of Kvasir-SEG. It shows that our model outputs better boundary and the prediction is more accurate.

Again, it shows that HarDNet[7] is a great and efficient backbone in not only classification and detection, but also medical imaging segmentation. We hope this study can help pushing the frontier of medical imaging and contribute to the application of CNN in this field.

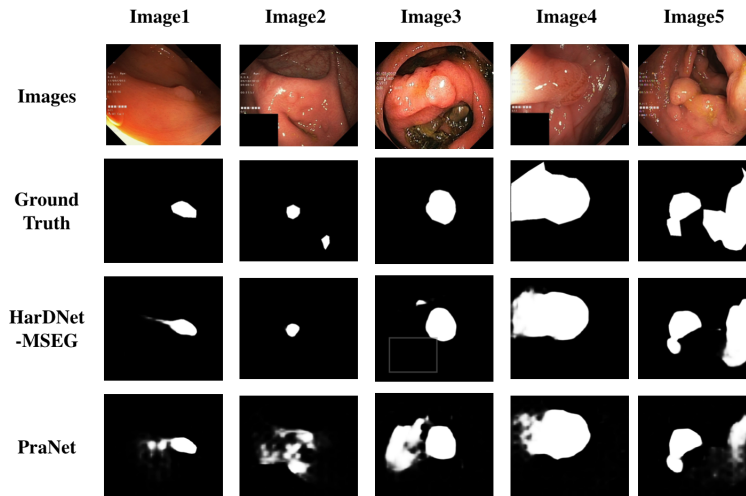


Figure 6: Inference results of Kvasir-SEG.

Acknowledgements

This research is supported in part by a grant from the Ministry of Science and Technology (MOST) of Taiwan. We thank National Center for High-performance Computing (NCHC) for providing computational and storage resources. Without it this research is impossible. We would also like to thank Mr.Ping Chao for many fruitful discussions.

References

- [1] Mojtaba Akbari, Majid Mohrekesh, Ebrahim Nasr-Esfahani, SM Reza Soroushmehr, Nader Karimi, Shadrokh Samavi, and Kayvan Najarian. Polyp segmentation in colonoscopy images using fully convolutional network. In *2018 40th Annual International Conference of the IEEE Engineering in Medicine and Biology Society (EMBC)*, pages 69–72. IEEE, 2018.
- [2] Mamonov A.V., Figueiredo I.N.and Figueiredo P.N., and Tsai Y.H.R. Automated polyp detection in colon capsule endoscopy. *IEEE TMI 33(7)*, 1488–1502, 2014.
- [3] Vijay Badrinarayanan, Alex Kendall, and Roberto Cipolla. Segnet: A deep convolutional encoder-decoder architecture for image segmentation. *IEEE transactions on pattern analysis and machine intelligence*, 39(12):2481–2495, 2017.
- [4] Seung-Hwan Bae and Kuk-Jin Yoon. Polyp detection via imbalanced learning and discriminative feature learning. *IEEE TMI 34(11)*, 2379–2393, 2015.
- [5] Jorge Bernal, F Javier Sánchez, Gloria Fernández-Esparrach, Debora Gil, Cristina Rodríguez, and Fernando Vilariño. Wm-dova maps for accurate polyp highlighting in colonoscopy: Validation vs. saliency maps from physicians. *Computerized Medical Imaging and Graphics*, 43:99–111, 2015.
- [6] Patrick Brandao, Evangelos Mazomenos, Gastone Ciuti, Renato Calì, Federico Bianchi, Arianna Menciassi, Paolo Dario, Anastasios Koulaouzidis, Alberto Arezzo, and Danail Stoyanov. Fully convolutional neural networks for polyp segmentation in colonoscopy. In *Medical Imaging 2017: Computer-Aided Diagnosis*, volume 10134, page 101340F. International Society for Optics and Photonics, 2017.
- [7] Ping Chao, Chao-Yang Kao, Yu-Shan Ruan, Chien-Hsiang Huang, and Youn-Long Lin. Hardnet: A low memory traffic network. In *Proceedings of the IEEE International Conference on Computer Vision*, pages 3552–3561, 2019.

- [8] Liang-Chieh Chen, Yi Yang, Jiang Wang, Wei Xu, and Alan L Yuille. Attention to scale: Scale-aware semantic image segmentation. In *Proceedings of the IEEE conference on computer vision and pattern recognition*, pages 3640–3649, 2016.
- [9] Liang-Chieh Chen, Yukun Zhu, George Papandreou, Florian Schroff, and Hartwig Adam. Encoder-decoder with atrous separable convolution for semantic image segmentation. In *Proceedings of the European conference on computer vision (ECCV)*, pages 801–818, 2018.
- [10] Long Chen, Hanwang Zhang, Jun Xiao, Liqiang Nie, Jian Shao, Wei Liu, and Tat-Seng Chua. Sca-cnn: Spatial and channel-wise attention in convolutional networks for image captioning. In *Proceedings of the IEEE conference on computer vision and pattern recognition*, pages 5659–5667, 2017.
- [11] Marius Cordts, Mohamed Omran, Sebastian Ramos, Timo Rehfeld, Markus Enzweiler, Rodrigo Benenson, Uwe Franke, Stefan Roth, and Bernt Schiele. The cityscapes dataset for semantic urban scene understanding. In *Proceedings of the IEEE conference on computer vision and pattern recognition*, pages 3213–3223, 2016.
- [12] Jia Deng, Wei Dong, Richard Socher, Li-Jia Li, Kai Li, and Li Fei-Fei. Imagenet: A large-scale hierarchical image database. In *2009 IEEE conference on computer vision and pattern recognition*, pages 248–255. Ieee, 2009.
- [13] Deng-Ping Fan, Ge-Peng Ji, Tao Zhou, Geng Chen, Huazhu Fu, Jianbing Shen, and Ling Shao. Pranet: Parallel reverse attention network for polyp segmentation. *MICCAI*, 2020.
- [14] Yuqi Fang, Delong Zhu, Jianhua Yao, Yixuan Yuan, and Kai-yu Tong. Abcnet: Area-boundary constraint network with dynamical feature selection for colorectal polyp segmentation. *IEEE Sensors Journal*, 2020.
- [15] Jun Fu, Jing Liu, Haijie Tian, Yong Li, Yongjun Bao, Zhiwei Fang, and Hanqing Lu. Dual attention network for scene segmentation. In *Proceedings of the IEEE Conference on Computer Vision and Pattern Recognition*, pages 3146–3154, 2019.
- [16] Kaiming He, Xiangyu Zhang, Shaoqing Ren, and Jian Sun. Spatial pyramid pooling in deep convolutional networks for visual recognition. *IEEE transactions on pattern analysis and machine intelligence*, 37(9):1904–1916, 2015.
- [17] Kaiming He, Xiangyu Zhang, Shaoqing Ren, and Jian Sun. Deep residual learning for image recognition. In *Proceedings of the IEEE conference on computer vision and pattern recognition*, pages 770–778, 2016.
- [18] Gao Huang, Zhuang Liu, Laurens Van Der Maaten, and Kilian Q Weinberger. Densely connected convolutional networks. In *Proceedings of the*

- IEEE conference on computer vision and pattern recognition*, pages 4700–4708, 2017.
- [19] Tajbakhsh N. and Gurudu S.R. and Liang J. Automated polyp detection in colonoscopy videos using shape and context information. *IEEE TMI* 35(2), 630–644, 2015.
- [20] Debesh Jha, Sharib Ali, Håvard D Johansen, Dag D Johansen, Jens Rittscher, Michael A Riegler, and Pål Halvorsen. Real-time polyp detection, localisation and segmentation in colonoscopy using deep learning. *arXiv preprint arXiv:2011.07631*, 2020.
- [21] Debesh Jha, Michael A Riegler, Dag Johansen, Pål Halvorsen, and Håvard D Johansen. Doubleu-net: A deep convolutional neural network for medical image segmentation. *arXiv preprint arXiv:2006.04868*, 2020.
- [22] Debesh Jha, Pia H Smedsrud, Michael A Riegler, Pål Halvorsen, Thomas de Lange, Dag Johansen, and Håvard D Johansen. Kvasir-seg: A segmented polyp dataset. In *International Conference on Multimedia Modeling*, pages 451–462. Springer, 2020.
- [23] Debesh Jha, Pia H Smedsrud, Michael A Riegler, Dag Johansen, Thomas De Lange, Pål Halvorsen, and Håvard D Johansen. Resunet++: An advanced architecture for medical image segmentation. In *2019 IEEE International Symposium on Multimedia (ISM)*, pages 225–2255. IEEE, 2019.
- [24] Nicolas Boutry Le Duy Huynh. A u-net++ with pre-trained efficientnet backbone for segmentation of diseases and artifacts in endoscopy images and videos. *ISBI 2020*, 2020.
- [25] Yann LeCun et al. Lenet-5, convolutional neural networks. *URL: <http://yann.lecun.com/exdb/lenet>*, 20(5):14, 2015.
- [26] Songtao Liu, Di Huang, et al. Receptive field block net for accurate and fast object detection. In *Proceedings of the European Conference on Computer Vision (ECCV)*, pages 385–400, 2018.
- [27] Jonathan Long, Evan Shelhamer, and Trevor Darrell. Fully convolutional networks for semantic segmentation. In *Proceedings of the IEEE conference on computer vision and pattern recognition*, pages 3431–3440, 2015.
- [28] Ahmed Mohammed, Sule Yildirim, Ivar Farup, Marius Pedersen, and Øistein Hovde. Y-net: A deep convolutional neural network for polyp detection. *arXiv preprint arXiv:1806.01907*, 2018.
- [29] Olaf Ronneberger, Philipp Fischer, and Thomas Brox. U-net: Convolutional networks for biomedical image segmentation. In *International Conference on Medical image computing and computer-assisted intervention*, pages 234–241. Springer, 2015.

- [30] Juan Silva, Aymeric Histace, Olivier Romain, Xavier Dray, and Bertrand Granado. Toward embedded detection of polyps in wce images for early diagnosis of colorectal cancer. *International Journal of Computer Assisted Radiology and Surgery*, 9(2):283–293, 2014.
- [31] David Vázquez, Jorge Bernal, F Javier Sánchez, Gloria Fernández-Esparrach, Antonio M López, Adriana Romero, Michal Drozdal, and Aaron Courville. A benchmark for endoluminal scene segmentation of colonoscopy images. *Journal of healthcare engineering*, 2017, 2017.
- [32] Zhe Wu, Li Su, and Qingming Huang. Cascaded partial decoder for fast and accurate salient object detection. In *Proceedings of the IEEE Conference on Computer Vision and Pattern Recognition*, pages 3907–3916, 2019.
- [33] Xiaofei Yang, Xutao Li, Yunming Ye, Raymond YK Lau, Xiaofeng Zhang, and Xiaohui Huang. Road detection and centerline extraction via deep recurrent convolutional neural network u-net. *IEEE Transactions on Geoscience and Remote Sensing*, 57(9):7209–7220, 2019.
- [34] Fisher Yu, Dequan Wang, Evan Shelhamer, and Trevor Darrell. Deep layer aggregation. In *Proceedings of the IEEE conference on computer vision and pattern recognition*, pages 2403–2412, 2018.
- [35] Jiafu Zhong, Wei Wang, Huisi Wu, Zhenkun Wen, and Jing Qin. Polypseg: An efficient context-aware network for polyp segmentation from colonoscopy videos. In *International Conference on Medical Image Computing and Computer-Assisted Intervention*, pages 285–294. Springer, 2020.
- [36] Zongwei Zhou, Md Mahfuzur Rahman Siddiquee, Nima Tajbakhsh, and Jianming Liang. Unet++: A nested u-net architecture for medical image segmentation. In *Deep Learning in Medical Image Analysis and Multimodal Learning for Clinical Decision Support*, pages 3–11. Springer, 2018.